TISSUE ENGINEERING: Part A
Volume 15, Number 9, 2009

DOI: 10.1089/ten.tea.2008.0510

Original Article

Dose Effect of Dual Delivery of Vascular Endothelial Growth Factor and Bone Morphogenetic Protein-2 on Bone Regeneration in a Rat Critical-Size Defect Model

Simon Young, D.D.S., Ph.D.,[1] Zarana S. Patel, Ph.D.,[1] James D. Kretlow, B.S., B.A.,[1] Matthew B. Murphy, Ph.D.,[1] Paschalia M. Mountziaris, B.S.,[1] L. Scott Baggett, Ph.D.,[2] Hiroki Ueda, Ph.D.,[3] Yasuhiko Tabata, Ph.D., D.Med.Sci., D.Pharm.,[4] John A. Jansen, D.D.S, Ph.D.,[5] Mark Wong, D.D.S.,[6] and Antonios G. Mikos, Ph.D.[1]

The dose effect of dual delivery of vascular endothelial growth factor (VEGF) and bone morphogenetic protein-2 (BMP-2) on bone regeneration was investigated in a rat cranial critical-size defect (CSD). It was hypothesized that decreasing amounts of BMP-2 would result in a dose-dependent decrease in bone formation, and that this reduction in bone formation could be reversed by adding increasing amounts of VEGF. *In vitro* release kinetics of VEGF or BMP-2 were examined over 28 days. Next, scaffolds were implanted within a rat cranial CSD containing different combinations of both BMP-2 and VEGF. At 12 weeks, samples were analyzed using microcomputed tomography and histology. *In vitro*, VEGF and BMP-2 exhibited burst release in the first 24 h followed by a significant decrease in release rate over 27 days. Overall, BMP-2 had a more sustained release versus VEGF. An *in vivo* dose-dependent decrease in percentage of bone fill (PBF) was observed for BMP-2. The addition of VEGF was unable to reverse this decrease in PBF, although improvements in the number of bridged defects did occur in some groups. This suggests that for this particular model simultaneous release of BMP-2 and VEGF does not increase bone formation over BMP-2 alone at 12 weeks.

Introduction

Bone healing is typically a highly efficient process that allows for the scarless regeneration and remodeling of defects related to the treatment of trauma, pathology, or congenital abnormalities. While standard techniques of reduction and fixation rely on the body's natural healing capacity for the treatment of most fractures, more extensive bone defects may require the use of bone grafting procedures to help augment the chances of a successful treatment outcome. Autologous bone still remains the gold-standard reconstructive material for many surgeons, although additional time, cost, and potential morbidity are associated with harvesting procedures. This has driven research in the field of tissue engineering to explore alternatives that utilize a variety of biomaterials (natural polymers,[1–3] synthetic polymers,[4–6] metals,[6–8] or ceramics[9–11]), bioactive factors (bone morphogenetic proteins [BMPs],[12] fibroblast growth factor-2 [FGF-2],[13] platelet-derived growth factor,[14] thrombin peptide 508,[15] transforming growth factor beta [TGF-β],[16] or vascular endothelial growth factor [VEGF][17]), and cell populations (bone marrow–derived,[18] muscle-derived,[19] or adipose-derived stem cells[20]) either alone or in combination.

Regardless of the approach employed, adequate vascularization of any bone tissue engineering construct of appreciable size is critical for cell survival and tissue function, because the diffusion of oxygen and nutrients through tissue is limited to a distance of approximately 150–200 μm.[21–23] In addition to the physiologic maintenance of any tissue-engineered graft material, neovascularization is crucial to both intramembranous[24] and endochondral[25] bone formation during development, and fracture healing as well.[26] As such, regenerative strategies attempting to recapitulate the sequence of key growth factors seen during bone healing

[1]Departments of Bioengineering and [2]Statistics, Rice University, Houston, Texas.
[3]School of Pharmacy, Hyogo University of Health Sciences, Chuo-ku, Kobe, Japan.
[4]Department of Biomaterials, Field of Tissue Engineering, Institute for Frontier Medical Sciences, Kyoto University, Sakyo-ku, Kyoto, Japan.
[5]Department of Periodontology and Biomaterials, Radboud University Nijmegen Medical Center, Nijmegen, The Netherlands.
[6]Department of Oral and Maxillofacial Surgery, University of Texas Health Science Center at Houston, Houston, Texas.

should promote the establishment of an adequate vascularized bed for subsequent bone formation.

VEGF is one among a host of angiogenic growth factors that have been evaluated for their effectiveness in bone tissue engineering models.[27] VEGF plays an essential role in neovascularization and has been shown to modulate endothelial cell proliferation, migration, and tube formation.[28,29] While VEGF was originally presumed to be highly selective for endothelial cells, the presence of VEGF receptors has been demonstrated on osteoblastic cells.[30] Additionally, VEGF has been shown to be a chemoattractant for both osteoblasts and endothelial cells,[31] and also a stimulant of osteoblast differentiation.[30]

The pleiotropic effects of VEGF have prompted studies investigating the role of VEGF as a coupling factor for angiogenesis and bone formation. Street *et al.*[32] inhibited VEGF activity in both a femoral fracture and a tibial cortical defect model using a soluble, neutralizing VEGF receptor. Bone repair was disrupted in both cases. This suggests that endogenous VEGF plays a role in the conversion of the cartilaginous soft callus to a hard, mineralized callus in long bone fracture repair, similar to its involvement in blood vessel invasion of the hypertrophic cartilage layer and subsequent ossification of the growth plate during development. This also implies that VEGF is involved in intramembranous ossification possibly through the stimulation of osteoblast chemotaxis and differentiation, and the recruitment of osteoblastic progenitor cells delivered to the wound by neovascularization.

The considerable role played by VEGF in osteogenesis has prompted a number of studies to examine the relationship of VEGF to one of the most widely studied growth factors in bone formation—bone morphogenetic protein-2 (BMP-2). Sipola *et al.*[33] found that endostatin, a natural antagonist of VEGF, abrogated BMP-2–induced ectopic bone formation in a mouse muscle pouch model. Similarly, Peng *et al.*[34] investigated the effect of the VEGF antagonist soluble fms-like tyrosine kinase 1 (sFlt1) on BMP-2–induced bone formation and healing. The authors found that sFlt1 significantly inhibited angiogenesis, delayed hypertrophic cartilage resorption, and inhibited the mineralized bone formation associated with BMP-2 delivery, indicating that endogenous VEGF activity is important to BMP-2–induced bone formation. In addition, exogenous VEGF delivery was found to enhance BMP-2–induced bone healing through increased angiogenesis and accelerated cartilage resorption and mineralization.

Aside from the previously mentioned synergistic actions of VEGF and BMP-2 on bone healing, VEGF and hypoxia have been shown to upregulate BMP-2 mRNA and protein expression in endothelial cells,[35] while hypoxia and BMPs have been shown to increase VEGF expression in osteoblasts.[36,37] Thus, both VEGF and BMP-2 may act as key mediators in a complex, reciprocal fracture repair signaling loop involving endothelial cells and osteoblasts.[35]

A number of studies have utilized methods of controlled release to deliver either VEGF[17,32,38,39] or BMP-2[3,40–42] to enhance bone healing in animal models. However, Simmons *et al.*[43] have noted that because bone formation and repair are controlled by many regulatory signals, it may be necessary to deliver multiple growth factors in specific combinations for effective tissue regeneration. Few studies have examined the *in vivo* effect of VEGF and BMP-2 combined delivery on bone regeneration in an orthotopic site. Peng *et al.*[34] used *ex vivo* gene therapy to create muscle-derived stem cells (MDSCs) expressing either BMP-2 or VEGF. Implantation of collagen scaffolds impregnated with both BMP-2–expressing and VEGF-expressing MDSCs was found to regenerate significantly more bone in a 6 mM calvarial rat defect than scaffolds containing VEGF-expressing MDSCs alone. In addition, the BMP-2+ VEGF group had significantly higher bone density than the group containing BMP-2–expressing cells only.

To our knowledge, only one study has examined the effect of simultaneous, controlled release of VEGF and BMP-2 proteins in an orthotopic bone model. Patel *et al.*[44] utilized a rat cranial critical-size defect (CSD) model to evaluate the angiogenic and osteogenic response to porous poly(propylene fumarate) (PPF) scaffolds incorporating gelatin microparticles (GMPs) for the controlled release of either VEGF (12 μg) alone, BMP-2 (2 μg) alone, or both VEGF (12 μg) and BMP-2 (2 μg). At 4 weeks postimplantation, the dual release group exhibited significantly more bone formation than the other groups. By 12 weeks postimplantation, both the BMP-2 and VEGF + BMP-2 groups showed significantly more bone formation than the empty control and the VEGF-only groups, although the VEGF + BMP-2 group was no longer statistically significantly different from the BMP-2 group. These results suggest that for the particular controlled release system and growth factor doses chosen, the beneficial effect of combined delivery of VEGF and BMP-2 peaked between 4 and 12 weeks, allowing the single delivery of BMP-2 to equalize by 12 weeks.

The aim of the present study was to examine the osteogenic response to varied doses of both VEGF and BMP-2, simultaneously delivered within a rat cranial CSD over 12 weeks. Previous studies have shown a minimal effect of growth factor dose on *in vitro* release kinetics for VEGF[45] and BMP-2[46] amounts in the range of 6–60 ng/mg of GMPs. In support of the planned *in vivo* work for this current study, radiolabeled VEGF (4.8 μg/mg GMP) or BMP-2 (0.8 μg/mg GMP) were loaded into both GMPs alone and porous PPF/GMP constructs to examine if *in vitro* release kinetics would be affected using the much larger growth factor loading doses of relevance to *in vivo* work.

Specifically, it was hypothesized that decreased amounts of BMP-2 from previous *in vivo* work (0.5–1 μg in this study vs. 2 μg previously)[44] would result in a dose-dependent decrease in bone formation in the BMP-2-only control groups, and that this reduction in bone formation could be reversed by the addition of increasing amounts of VEGF (0.5–1 μg). To test this hypothesis, a controlled release system composed of a porous PPF scaffold incorporating GMPs was chosen. This system has been utilized previously for bone tissue engineering purposes[44] and relies on acidic GMPs crosslinked with 10 mM glutaraldehyde for VEGF release[45] and basic GMPs crosslinked with 40 mM glutaraldehyde for BMP-2 release.[46] These composite scaffolds were implanted in a rat cranial CSD and examined by microcomputed tomography (micro-CT) and histology at 12 weeks postimplantation so that the results could be directly compared to previous work in this laboratory.[44]

Materials and Methods

Experimental design

For the first part of this study, the *in vitro* release kinetics of VEGF and BMP-2 from GMPs alone and porous PPF scaffolds incorporating GMPs were evaluated (Table 1).

Based on previous optimization studies in our lab,[45,46] acidic GMPs with an isoelectric point (IEP) of 5 and crosslinked with 10 mM glutaraldehyde were chosen for the controlled release of VEGF (IEP = 8.6), and basic GMPs with an IEP of 9 and crosslinked with 40 mM glutaraldehyde were chosen for the controlled release of BMP-2 (IEP = 8.5). This resulted in the following four groups ($n = 3$ each): GMPs loaded with 6 μg VEGF (Group G/V), porous PPF scaffolds incorporating GMPs loaded with 6 μg VEGF (Group PG/V), GMPs loaded with 1 μg BMP-2 (Group G/B), and porous PPF scaffolds incorporating GMPs loaded with 1 μg BMP-2 (Group PG/B). All samples were incubated in phosphate buffered saline (PBS) containing 400 ng/mL of bacterial collagenase 1A, an enzyme that is known to digest gelatin.[47]

The second part of this study evaluated the *in vivo* dose effects of VEGF and BMP-2 on bone formation. The experimental groups (Table 1) consisted of porous PPF scaffolds incorporating GMPs loaded with a range of VEGF and BMP-2 doses, specifically resulting in the following (each with $n = 8$): 1 μg BMP-2 (0.02 μg/mm^3) + 6 μg VEGF (0.12 μg/mm^3) (Group 1B/6V); 1 μg BMP-2 (0.02 μg/mm^3) + 12 μg VEGF (0.24 μg/mm^3) (Group 1B/12V); 0.5 μg BMP-2 (0.01 μg/mm^3) + 6 μg VEGF (0.12 μg/mm^3) (Group 0.5B/6V); and 0.5 μg BMP-2 (0.01 μg/mm^3) + 12 μg VEGF (0.24 μg/mm^3) (Group 0.5B/12V). Controls consisted of single growth factor delivery of BMP-2 only, resulting in the following (each with $n = 8$): 1 μg BMP-2 (0.02 μg/mm^3) (Group 1B/0V) and 0.5 μg BMP-2 (0.01 μg/mm^3) (Group 0.5B/0V). These amounts were chosen so that the dose effects could be directly compared to previous work in our laboratory that delivered either no growth factor (Group 0B/0V), 2 μg BMP-2 (0.04 μg/mm^3) (Group 2B/0V), 12 μg VEGF (0.24 μg/mm^3) (Group 0B/12V), or 2 μg BMP-2 (0.04 μg/mm^3) + 12 μg VEGF (0.24 μg/mm^3) (Group 2B/12V) from the same controlled release system.[44] All scaffolds were implanted into rat cranial CSDs for a period of 12 weeks, scanned by micro-CT after harvest, and finally sectioned for histological analysis.

PPF synthesis and porous PPF scaffold fabrication

PPF was synthesized in a two-step process according to previous methods.[48,49] PPF structure was confirmed by ^{1}H nuclear magnetic resonance. Gel permeation chromatography (Waters, Milford, MA) indicated a PPF number average molecular weight (M_n) of 2064 and polydispersity index of 1.78 relative to polystyrene standards (Fluka, Buchs, Switzerland).

Porous polymer scaffolds (8 mm diameter, 1 mm height) made from a 1:1 mass ratio mixture of PPF and N-vinyl pyrrolidone with 80 wt% NaCl (300–500 μm crystals) included as a porogen were fabricated and leached in deionized, distilled water as previously described.[44] All scaffolds were then flushed with 70% ethanol and lyophilized overnight. Scaffolds to be used for the *in vivo* study were subsequently sterilized in ethylene oxide gas for 24 h.

GMP fabrication

Microparticles with a size range of 50–100 μm were made from gelatin (Nitta Gelatin Co., Osaka, Japan), crosslinked in glutaraldehyde solution, and lyophilized as previously described.[44]

Acidic GMPs were crosslinked with 10 mM glutaraldehyde and used for VEGF release, while basic GMPs were crosslinked with 40 mM glutaraldehyde and used for BMP-2 release. For the *in vivo* study, diffusional loading was used to incorporate the growth factors into the lyophilized GMPs: a solution of growth factor in PBS (0.16 mg/mL BMP-2 [Peprotech, Rocky Hill, NJ] or 0.96 mg/mL VEGF [Peprotech]) was dripped onto the GMPs at a volume of 5 μL/mg of microparticles. After vortexing, the loaded microparticles were incubated for 20 h at 4°C. For the *in vitro* study, the same concentrations of growth factor solution were used for diffusional loading; however, radiolabeled growth factors were incorporated as well (please refer to the *In vitro* release study section).

Table 1. Description of the Amount of Bone Morphogenic Protein-2 (0, 0.5, 1, or 2 μg) and Vascular Endothelial Growth Factor (0, 6, or 12 μg) Used in Each Experimental Group Within This Study and Patel *et al.*[44]

Group	*BMP dose (μg)*	*VEGF dose (μg)*	*Construct*	*Study*
In vitro *study groups*				
Group G/V	0	6	GMPs only	Current study
Group G/B	1	0	GMPs only	Current study
Group PG/V	0	6	PPF w/GMPs	Current study
Group PG/B	1	0	PPF w/GMPs	Current study
In vivo *study groups*				
Group 0B/0V	0	0	PPF w/GMPs	Patel *et al.*
Group 0B/12V	0	12	PPF w/GMPs	Patel *et al.*
Group 0.5B/0V	0.5	0	PPF w/GMPs	Current study
Group 0.5B/6V	0.5	6	PPF w/GMPs	Current study
Group 0.5B/12V	0.5	12	PPF w/GMPs	Current study
Group 1B/0V	1	0	PPF w/GMPs	Current study
Group 1B/6V	1	6	PPF w/GMPs	Current study
Group 1B/12V	1	12	PPF w/GMPs	Current study
Group 2B/0V	2	0	PPF w/GMPs	Patel *et al.*
Group 2B/12V	2	12	PPF w/GMPs	Patel *et al.*

The type of construct used for each group is also shown (either GMPs only, or PPF scaffold/GMP composites).

BMP, bone morphogenic protein; VEGF, vascular endothelial growth factor; GMP, gelatin microparticle; PPF, porous poly(propylene fumarate).

Composite scaffold generation

To generate composite scaffolds, all porous PPF scaffolds received 2.5 mg each of acidic and basic GMPs, premixed together in 30 μL of a 24% aqueous solution of Pluronic F-127 (Sigma-Aldrich, St. Louis, MO). After injection of the GMPs into the pores of the PPF scaffolds, the incorporated mixture was allowed to gel at room temperature for 10 min. Depending on the experimental group, various doses of VEGF (0, 6, or 12 μg), BMP-2 (0.5 or 1 μg), and blank PBS-loaded GMPs were incorporated into the composite scaffolds. However, the loading concentration of growth factor per mg of GMP was always kept constant—that is, a VEGF loading dose of 4.8 μg/mg of 10 mM acidic GMPs and a BMP-2 loading dose of 0.8 μg/mg of 40 mM basic GMPs (Table 2). Thus, the dose of VEGF and BMP-2 per scaffold was varied by controlling the ratio of loaded to unloaded GMPs.

In vitro *release study*

Preparation of radiolabeled VEGF solution. The VEGF loading solution for the *in vitro* release work consisted of a mixture of radiolabeled and unlabeled growth factor in a mass ratio of 0.0005:1. Radiolabeled VEGF (radioiodinated with ^{125}I using a modification of the iodogen method) was purchased from PerkinElmer (Waltham, MA), and unlabeled VEGF was obtained from Peprotech.

Preparation of radiolabeled BMP-2 solution. BMP-2 (Astellas Pharma, Inc., Tokyo, Japan) was radioiodinated using the chloramine-T method of Greenwood *et al*.[50] Briefly, 4 mL of NaI^{125} was added to a 40 mL solution of BMP-2 (3 mg/mL) containing 5 mM glutamic acid, 2.5 wt% glycine, 0.5 wt% sucrose, and 0.01 wt% Tween 80 (pH 4.5). About 100 μL of chloramine-T (0.2 mg/mL) (Nacalai Tesque, Inc., Kyoto, Japan) in a 0.5 M potassium phosphate-buffered solution containing 0.5 M NaCl (pH 7.5) was then added. After agitation of the mixture for 2 min at room temperature, 100 μL of PBS containing 0.4 mg sodium metabisulfate was used to terminate the reaction. Gel filtration through a Sephadex PD-10 column (Amersham Biosciences, Pittsburg, PA) was used to purify the solution and remove any free I^{125} remaining. The concentration of BMP-2 was then determined using a bicinchoninic acid protein assay (Pierce Biotechnologies, Rockford, IL).

Measurement of *in vitro* release kinetics. Preparation of radiolabeled growth factor solutions and growth factor loading of the GMPs to generate groups G/V, PG/V, and G/B, and PG/B were achieved as described above. GMPs alone or composite scaffolds composed of porous PPF incorporating GMPs were incubated in 400 ng/mL collagenase type 1A buffer at 37°C under shaking at 70 rpm. At each time point (days 0.5, 1, 2, 3, 6, 9, 13, 16, 20, 24, and 28), the buffer was removed and replaced with fresh buffer. For groups G/V, G/B, and PG/B, the samples were centrifuged for 5 min at 3000 rpm before buffer extraction so that the loss of microparticles during buffer removal was minimized. Standards containing known amounts of radiolabeled growth factor were used to account for radioactive decay. The release of radiolabeled growth factor into the surrounding buffer was quantified using a gamma counter (Cobra II Autogamma [Packard, Meridian, CT] for VEGF release, and ARC-301B [Aloka Co., Tokyo, Japan] for BMP-2 release), and the results were correlated to a standard curve. The percent cumulative release of growth factor at each time point was determined as follows:

$$\%\,\text{Cumulative release at time } X = \frac{\sum \text{Growth factor released up to time } X}{(\sum \text{Growth factor released over entire study}) + \text{growth factor remaining in sample at last time}}$$

Table 2. Growth Factor and Gelatin Microparticle Composition in Each Group

Group	*BMP-2–loaded 40 mM basic GMP (mg)*	*PBS-loaded 40 mM basic GMP (mg)*	*VEGF-loaded 10 mM acidic GMP (mg)*	*PBS-loaded 10 mM acidic GMP (mg)*
In vitro *study groups*				
Group G/V	0	2.5	1.25	1.25
Group G/B	1.25	1.25	0	2.5
Group PG/V	0	2.5	1.25	1.25
Group PG/B	1.25	1.25	0	2.5
In vivo *study groups*				
Group 0B/0V	0	0	0	0
Group 0B/12V	0	2.5	2.5	0
Group 0.5B/0V	0.63	1.88	0	2.5
Group 0.5B/6V	0.63	1.88	1.25	1.25
Group 0.5B/12V	0.63	1.88	2.5	0
Group 1B/0V	1.25	1.25	0	2.5
Group 1B/6V	1.25	1.25	1.25	1.25
Group 1B/12V	1.25	1.25	2.5	0
Group 2B/0V	2.5	0	0	2.5
Group 2B/12V	2.5	0	2.5	0

As discussed in the Materials and Methods, to keep the GMP growth factor loading concentration consistent, 5 μL of growth factor solution (either 0.16 mg/mL BMP-2 or 0.96 mg/mL VEGF) was used for every mg of microparticles. Thus, growth factor dose was controlled by varying the amount of growth factor–loaded GMPs incorporated into each group. In addition, it was ensured that the total amount of GMPs incorporated in each group remained consistent at 5 mg (except the control Group 0B/0V). The exact combination of microparticles used for each group is shown below. PBS, phosphate buffered saline.

Release rates were calculated as the slope of % cumulative release over the stated time period and are reported as change in % cumulative release per day.

In vivo *dose effect study*

Animal surgery, euthanasia, and implant retrieval. This work was conducted in accordance with protocols approved by the Rice University Institutional Animal Care and Use Committee. Before surgery, all materials designated for implantation were sterilized using ethylene oxide (GMPs, porous PPF scaffolds, and dry Pluronic F-127) or 0.22 μm syringe filters (water and PBS). GMP loading and composite scaffold generation were all carried out under sterile conditions before surgical implantation.

Forty-eight healthy male syngeneic Fischer 344 rats (12 weeks old and weighing 175–225 g) were purchased from Harlan (Indianapolis, IN). General inhalational anesthesia, the creation of an 8-mm-diameter critical-size cranial defect, the placement of composite scaffolds in the defect site, and postoperative animal care were performed as previously described.[44] At 12 weeks postimplantation, the rats were euthanized, and the implants retrieved using established methods.[44]

Microcomputed tomography imaging—animal specimens. The harvested cranial bone defects were imaged using a high-resolution SkyScan-1172 micro-CT imaging system (SkyScan, Aartselaar, Belgium). Each specimen was fixed vertically by the sample holder and placed in the micro-CT specimen chamber. The scanner was set to a nominal resolution of 10 μm/pixel, and based on the manufacturer's recommendations along with previous studies,[44] voltage was set at 100 kV and current at 100 μA with a 0.5 mM aluminum filter in place. Resolution was set to high, which created 1280×1024 raw images, and frame averaging was set to 4 frames per view to increase the signal-to-noise ratio. Serial coronally oriented tomograms were reconstructed from the raw images in the NRecon CT Reconstruction software package (SkyScan) using a 3D cone beam reconstruction algorithm for back projection and convolution adapted from Feldkamp *et al.*[51]

Microcomputed tomography analysis—animal specimens. The coronally oriental tomograms were then reformatted in an axial orientation using CT-Analyzer (SkyScan) to facilitate the creation of an 8-mm-diameter, 1.5-mm-thick cylindrical volume of interest (VOI), which recreated the geometry of the original cylindrical defect made by the trephine drill. Thresholding analysis was conducted to optimize the parameters necessary for accurate binarization of samples. In brief, the lower binarization threshold index value was varied between 40 and 120, while the upper binarization threshold index value was held constant at 255. Lower and upper threshold indices of 70 and 255, respectively, were determined to be the values for which binarized tomograms most accurately represented their grayscale counterparts in terms of bone morphology. Thus, the percentage of bone volume within each cylindrical VOI was calculated as follows:

$$\%\ \text{Bone formation} = \frac{\text{Bone volume } (\mu m^3)}{\text{VOI volume } (\mu m^3)} \times 100\%$$

The extent of bony bridging and union within the defect was determined from the micro-CT datasets by generating maximum intensity projections (MIPs) for each sample in the CT-Analyzer software. Three blinded observers (J.D.K., P.M.M., and S.Y.) separately graded the MIPs according to the grading scale in Table 3 and reached a consensus score for each sample. Note that although the blinded observers who performed the MIP scoring in Patel *et al.*[44] (Zarana Patel and Simon Young) were different from this study (James Kretlow and Paschalia Mountziaris), the same quantitative scoring system was used.

Microcomputed tomography imaging—porous PPF scaffolds. Six 8-mm-diameter, 1-mm-thick porous PPF scaffolds were scanned using the SkyScan-1172 micro-CT imaging system. The manufacturer's recommended voltage of 40 kV and a current of 250 μA were utilized with no aluminum filter and a nominal resolution of 8 μm/pixel. Resolution was set to high, which created 1280×1024 raw images, and frame

Table 3. Scoring Guide for Extent of Bony Bridging and Union Using Maximum Intensity Projections of Microcomputed Tomography Datasets

Description	*Score*
Bony bridging over entire span of defect at longest point (8 mm)	4
Bony bridging over partial length of defect	3
Bony bridging only at defect borders	2
Few bony spicules dispersed throughout defect	1
No bone formation within defect	0

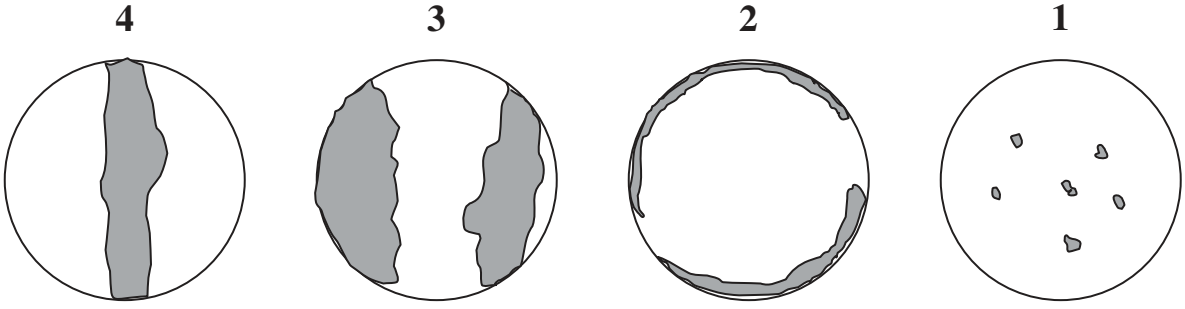

averaging was set to 4 to increase the signal-to-noise ratio. Serial tomograms were reconstructed from the raw images in NRecon using the Feldkamp 3D cone beam reconstruction algorithm for back projection and convolution.

Microcomputed tomography analysis—porous PPF scaffolds. Porous PPF scaffold cross sections generated by NRecon were all reformatted in CT-Analyzer in the correct orientation, which allowed for a cylindrical ROI to be used for analysis. Scaffolds were analyzed in CT-Analyzer for both porosity and pore interconnectivity using a global threshold of 50–255. Scaffold porosity was derived using CT-Analyzer to determine the binarized object volume (i.e., the actual polymer volume of each scaffold) within a VOI just enclosing the porous PPF scaffold:

$$\%\ \text{Scaffold porosity} = \left(1 - \frac{\text{Binarized object volume}}{\text{VOI volume}}\right) \times 100\%$$

Pore interconnectivity of porous PPF scaffolds was determined as previously described.[52] The micro-CT datasets were loaded and resized by half, resulting in a pixel resolution of 16 μm. A VOI was defined by again superimposing a cylinder just enclosing the scaffold volume.

For each scaffold, the VOI and binarized object volume were quantified (VOI_{pre} and OV_{pre}). A three-dimensional shrink wrap was then performed in CT-Analyzer. In a process akin to applying vacuum to a sponge covered in cellophane wrap, this operation continuously shrinks the VOI toward the surface of the binarized solid object from the outside in. This eliminates all void space from the shrinking VOI that is accessible through pore interconnects of a predefined size (CT-Analyzer allows for even multiples of the original voxel size). This analysis was performed at 2, 4, 6, 8, 10, 12, 14, 16, 18, 20, and 22 times the voxel size, and the shrunk VOI (VOI_{post}) was determined. The binarized solid object volume calculated after the shrink wrap operation was completed (OV_{post}) equaled OV_{pre} because no polymer was lost from the scaffold in this nondestructive technique. The percentage of volume inaccessible to the shrinking VOI was determined as:

$$\%\ \text{Inaccessible volume} = \frac{VOI_{post} - OV_{post}}{VOI_{pre} - OV_{pre}} \times 100\%$$

Histological processing

After micro-CT scanning, the samples were dehydrated in a graded series of ethanol (from 70% to 100%) and embedded in methylmethacrylate. Once polymerization was complete, a modified diamond saw technique[53] was used to make three 10-μm-thick coronal sections per sample. Each section was subsequently stained with methylene blue/basic fuschin.

Light microscopy and histological scoring

Each of the three sections per sample was evaluated separately by two blinded observers (J.D.K. and P.M.M.) using light microscopy. A quantitative grading scale was used to assess the quality of the scaffold–bone interface and the tissue response within the pores of the scaffold (Table 4). Once this had been completed, a consensus score was reached for each section, and the overall mean score for the group was calculated. The mean histological scores for the groups in this study (Groups 0.5B/0V, 0.5B/6V, 0.5B/12V, 1B/0V, 1B/6V, and 1B/12V) were compared against the mean histological scores for the groups scored by Patel *et al.*[44] (Groups 0B/0V, 0B/12V, 2B/0V, and 2B/12V). Note that although the blinded observers who performed the histological scoring in Patel *et al.*[44] (Zarana Patel and Simon Young) were different from this study (Paschalia Mountziaris and James Kretlow), the same quantitative scoring system was used.

Statistical methods

For evaluation of the *in vitro* VEGF and BMP-2 release rates, a repeated measures analysis of variance (ANOVA) was performed, followed by a Tukey's multiple comparison test to determine statistical significance with 95% confidence intervals ($p < 0.05$). Standard ANOVA was performed on the *in vivo* % bone formation and bone score data, followed by a Tukey's multiple comparisons test to determine statistical significance with 95% confidence intervals ($p < 0.05$).* A truncated regression and ordered logit analysis was per-

Table 4. Quantitative Histological Scoring Guide as Used in This Study and Patel *et al.*[44]

Description	*Score*
Hard tissue response at scaffold–bone interface	
Direct bone to implant contact without soft interlayer	4
Remodeling lacuna with osteoblasts and/or osteoclasts at surface	3
Majority of implant is surrounded by fibrous tissue capsule	2
Unorganized fibrous tissue (majority of tissue is not arranged as capsule)	1
Inflammation marked by an abundance of inflammatory cells and poorly organized tissue	0
Hard tissue response within the pores of the scaffold	
Tissue in pores is mostly bone	4
Tissue in pores consists of some bone within mature, dense fibrous tissue and/or a few inflammatory response elements	3
Tissue in pores is mostly immature fibrous tissue (with or without bone) with blood vessels and young fibroblasts invading the space with few macrophages present	2
Tissue in pores consists mostly of inflammatory cells and connective tissue components in between (with or without bone) OR the majority of the pores are empty or filled with fluid	1
Tissue in pores is dense and exclusively of inflammatory type (no bone present)	0

*Because responses were measured as percentages, results from the standard ANOVA were confirmed using a truncated ANOVA–type approach for the PBF and bone score data, and a log-transformed % response for the VEGF release data. The truncated ANOVA assumes responses to be in the range of 0–100, while standard or ordinary least squares ANOVA assumes that responses can be between negative to positive infinity. The results for both analyses were identical.

formed on the % bone formation and bone score data, respectively, to determine if the results from this current study could be compared to previous work performed by this laboratory.[44] The results are reported as means ± standard deviation for $n = 3$ for the *in vitro* studies and $n = 8$–9 for the *in vivo* studies.

Results

Porous PPF scaffolds

Quantitative micro-CT analysis was performed on reconstructed porous PPF scaffold datasets to determine morphological characteristics such as porosity and pore interconnectivity. Mean PPF scaffold porosity ($n = 8$) was found to be 77.9 ± 2.1%. Serial pore interconnectivity analysis was performed by examining the change in % inaccessible volume, as larger pore size cut-offs were selected (i.e., the smallest pore the VOI could shrink through was increased from 32, 64, 96, 128, 160, 192, 224, 256, 288, 320, up to 352 μm). Up to the 192-μm size cut-off, the % inaccessible pore volume of the scaffolds stayed below 2%. However, when the VOI shrink wrap algorithm was instructed to limit the size of the smallest pore it could penetrate to 224 μm or larger, the % inaccessible pore volume increased sharply to approximately 38% (Fig. 1).

In vitro *growth factor release kinetics*

In vitro release of VEGF or BMP-2 from GMPs alone and porous PPF scaffolds incorporating GMPs was evaluated within collagenase-containing PBS over 28 days (Figs. 2 and 3). As in previous studies,[45–47,54] the release profiles were split into four time segments to facilitate comparisons in release rates between Group G/V and Group PG/V, or Group G/B and Group PG/B: Phase 1 (the first 24 h), Phase 2 (days 1–3), Phase 3 (days 3–16), and Phase 4 (days 16–28) (Tables 5 and 6). The repeated measures ANOVA found that the type of release vehicle used (i.e., GMP only vs. composite scaffolds) had an overall significant effect on % cumulative release ($p = 0.0041$).

For VEGF, both G/V and PG/V exhibited a fairly large burst release in the first 24 h with G/V and PG/V releasing

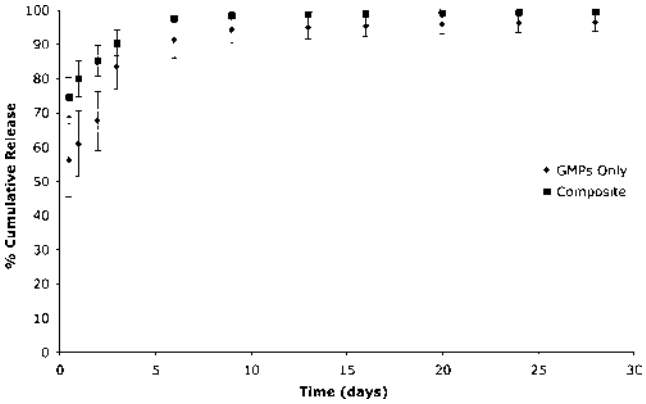

FIG. 2. Profile of the *in vitro* release of VEGF in collagenase buffer. Average percent cumulative VEGF release from GMPs only versus porous PPF scaffolds incorporating GMPs (composite). Error bars represent means ± standard deviation for $n = 3$.

60.7 ± 9.6% and 79.9 ± 5.1%, respectively (Fig. 2). This was followed by significantly reduced release rates thereafter (in Phases 2, 3, and 4): Group G/V exhibited VEGF release rates from 0.1% to 11%/day, while Group PG/V exhibited rates ranging from 0.0% to 5.2%/day. Between groups, only the Phase 1 and Phase 2 release rates were statistically significantly different. Within groups, for PG/V, Phase 1 was significantly different ($p < 0.05$) from each of the other phases, while Phases 2, 3, and 4 were not significantly different from each other. Both Phases 1 and 2 were significantly different from each of the other phases within group G/V.

BMP-2 did not exhibit the same large burst release profile as seen with VEGF in the first 24 h, as seen by comparison of Figures 2 and 3. In Phase 1, G/B and PG/B released BMP-2 at a rate of 2.8 ± 0.5% and 19.7 ± 8.0%, respectively. Subsequent release rates were significantly reduced, with G/B releasing BMP-2 at approximately 0.3%/day for the remainder of the study, while the release rates for Group PG/B in Phases 2–4 ranged from 0.5% to 2.0%/day. A statistically significant difference between groups was only found for the Phase 1

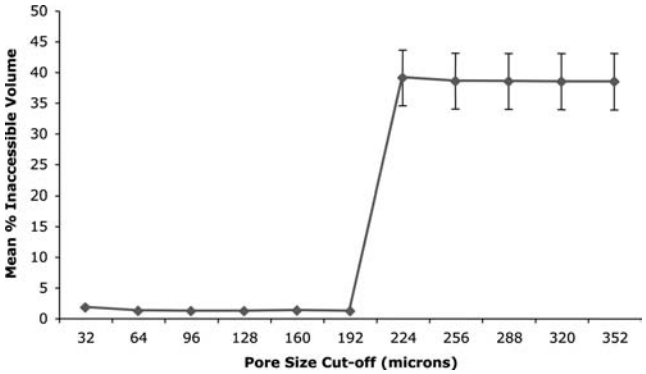

FIG. 1. Pore interconnectivity of porous PPF scaffolds, as measured by microcomputed tomography (micro-CT). The sudden increase in the percentage inaccessible volume between a 192 and 224 μm size cut-off indicates an average pore interconnect size within that range.

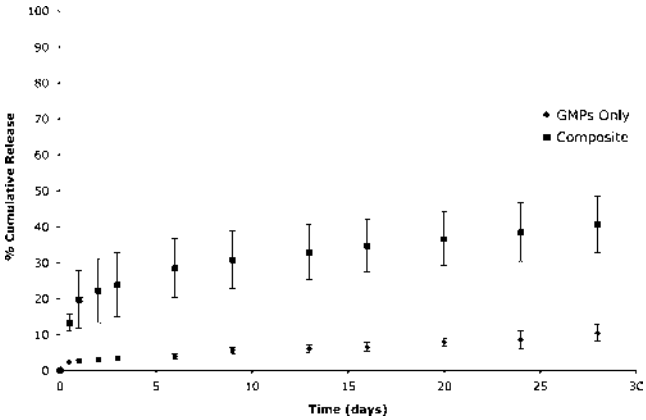

FIG. 3. Profile of the *in vitro* release of BMP-2 in collagenase buffer. Average percent cumulative BMP-2 release from GMPs only versus porous PPF scaffolds incorporating GMPs (composite). Error bars represent means ± standard deviation for $n = 3$.

Table 5. Release Kinetics of VEGF from GMPs Only and Composite Scaffolds

	Phase 1 (%/day) First 24 h	*Phase 2 (%/day) Days 1–3*	*Phase 3 (%/day) Days 3–16*	*Phase 4 (%/day) Days 16–28*
In vitro *VEGF release kinetics*				
Gelatin MPs	$60.7 \pm 9.6^{a,b}$	$11.3 \pm 1.5^{a,b}$	0.8 ± 0.3	0.1 ± 0.1
Composites	$79.9 \pm 5.1^{a,b}$	5.2 ± 0.7^{a}	0.5 ± 0.2	0.0 ± 0.0

Average percent values (% release per day) are given with standard deviations for $n = 3$.

[a]Statistical significance ($p < 0.05$) between groups for Phase (i.e., Phase 1, 2, 3, or 4).

[b]Within each group, a statistically significant difference ($p < 0.05$) of that particular phase from all other phases.

release rate. Within groups, PG/B's Phase 1 release rate was significantly different from all other phases, while none of the release rate phases for G/B were significantly different from each other.

In vivo *dose effects of BMP-2 and VEGF*

By integrating the healed area of each serial binarized tomogram throughout the defect volume, the percentage of bone fill (PBF) that had occurred within each group was determined (Fig. 4). The 12 week bone formation data from previous work (i.e., Groups 0B/0V, 0B/12V, 2B/0V, and 2B/12V)[44] were included for comparison, because truncated regression analysis showed that study (i.e., the previous work or this current work) had no significant effect on PBF, with $p = 0.6403$. As can be seen in Figure 4, the amount of bone formation exhibited by Groups 2B/0V ($37.4 \pm 18.8\%$) and 2B/12V ($39.7 \pm 14.1\%$) was statistically significantly different from all other groups.

Specifically, Groups 1B/0V ($19.4 \pm 7.5\%$) and 0.5B/0V ($6.2 \pm 4.9\%$) showed a statistically significant decrease in bone formation from Group 2B/0V, indicating a BMP-dose-dependent decrease in bone formation, although 1B/0V and 0.5B/0V were not statistically different from each other. A rescue effect of simultaneously adding VEGF was not observed in the groups that contained either 1 or 0.5 μg of BMP-2. Groups 1B/6V ($15.7 \pm 13.0\%$) and 1B/12V ($9.3 \pm 6.3\%$) were not significantly different from 1B/0V, nor were 0.5B/6V ($7.6 \pm 4.4\%$) and 0.5B/12V ($12.2 \pm 10.5\%$) significantly different from 0.5B/0V, indicating that the addition of 6 or 12 μg of VEGF to the BMP-only controls in this study did not result in a higher amount of bone formation at 12 weeks. While several groups in this current study displayed a higher mean PBF than the 0B/0V control group of the previous study[44] (i.e., Groups 0.5B/12V, 1B/0V, 1B/6V, and 1B/12V), the difference was not significant.

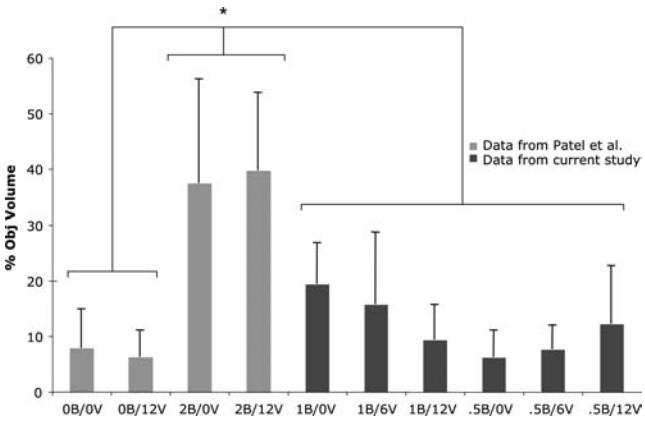

FIG. 4. Percent bone formation within the defect at 12 weeks as measured by micro-CT. Values are given for % bone formation of the groups performed by Patel *et al.*[44] (Groups 0B/0V, 0B/12V, 2B/0V, and 2B/12V) and this current study (Groups 1B/0V, 1B/6V, 1B/12V, 0.5B/0V, 0.5B/6V, and 0.5B/12V). Error bars represent means ± standard deviation for $n =$ 8–9. At 12 weeks, Groups 2B/0V and 2B/12V are statistically significantly different ($p < 0.05$) from all other groups, as denoted by asterisks (*).

An additional method of analysis used to assess bone healing was the scoring of bone formation by blinded observers shown maximum intensity projections of each animal (Fig. 5). The mean bone scores as seen in Figure 6 show that Groups 2B/0V (3.4 ± 0.5) and 2B/12V (3.6 ± 0.5) had a statistically significantly higher score than Groups 0B/0V (2.0 ± 1.1) and 0B/12V (2.0 ± 0.5) (as shown previously[44]), and that Groups 0.5B/0V (2.4 ± 0.7) and 0.5B/6V (2.4 ± 0.5) showed a statistically significant decrease in bone formation as compared to 2B/12V.

In terms of the number of samples that exhibited bony bridging within each group, a dose-dependent decrease was observed for BMP-2, such that Group 2B/0V had 3/8 samples bridged, while Groups 1B/0V and 0.5B/0V had 1/8 and 0/8 samples bridged, respectively. Further, the addition of VEGF seemed to increase the number of bridged samples per group in certain cases: Group 2B/12V versus Group 2B/0V (5/8 vs. 3/8 bridged), Group 1B/6V versus Group 1B/0V (3/8 vs. 1/8 bridged), and Group 0.5B/12V versus both Groups 0.5B/0V and 0.5B/6V (2/8 bridged vs. 0/8 bridged for both).

As an adjunct to micro-CT analysis, both qualitative (Fig. 7) and quantitative (Fig. 8) histological examinations of Groups 1B/0V, 1B/6V, 1B/12V, 0.5B/0V, 0.5B/6V, and 0.5B/12V were performed to characterize the tissue response at the scaffold–bone interface and within the pores of the

Table 6. Release Kinetics of BMP-2 from GMPs Only and Composite Scaffolds

	Phase 1 (%/day) First 24 h	*Phase 2 (%/day) Days 1–3*	*Phase 3 (%/day) Days 3–16*	*Phase 4 (%/day) Days 16–28*
In vitro *BMP-2 release kinetics*				
Gelatin MPs	2.8 ± 0.5^{a}	0.3 ± 0.1	0.2 ± 0.0	0.3 ± 0.2
Composites	$19.7 \pm 8.0^{a,b}$	2.0 ± 0.5	0.8 ± 0.1	0.5 ± 0.0

Average percent values (% release per day) are given with standard deviations for $n = 3$.

[a]Statistical significance ($p < 0.05$) between groups for Phase (i.e., Phase 1, 2, 3, or 4).

[b]Within each group, a statistically significant difference ($p < 0.05$) of that particular phase from all other phases.

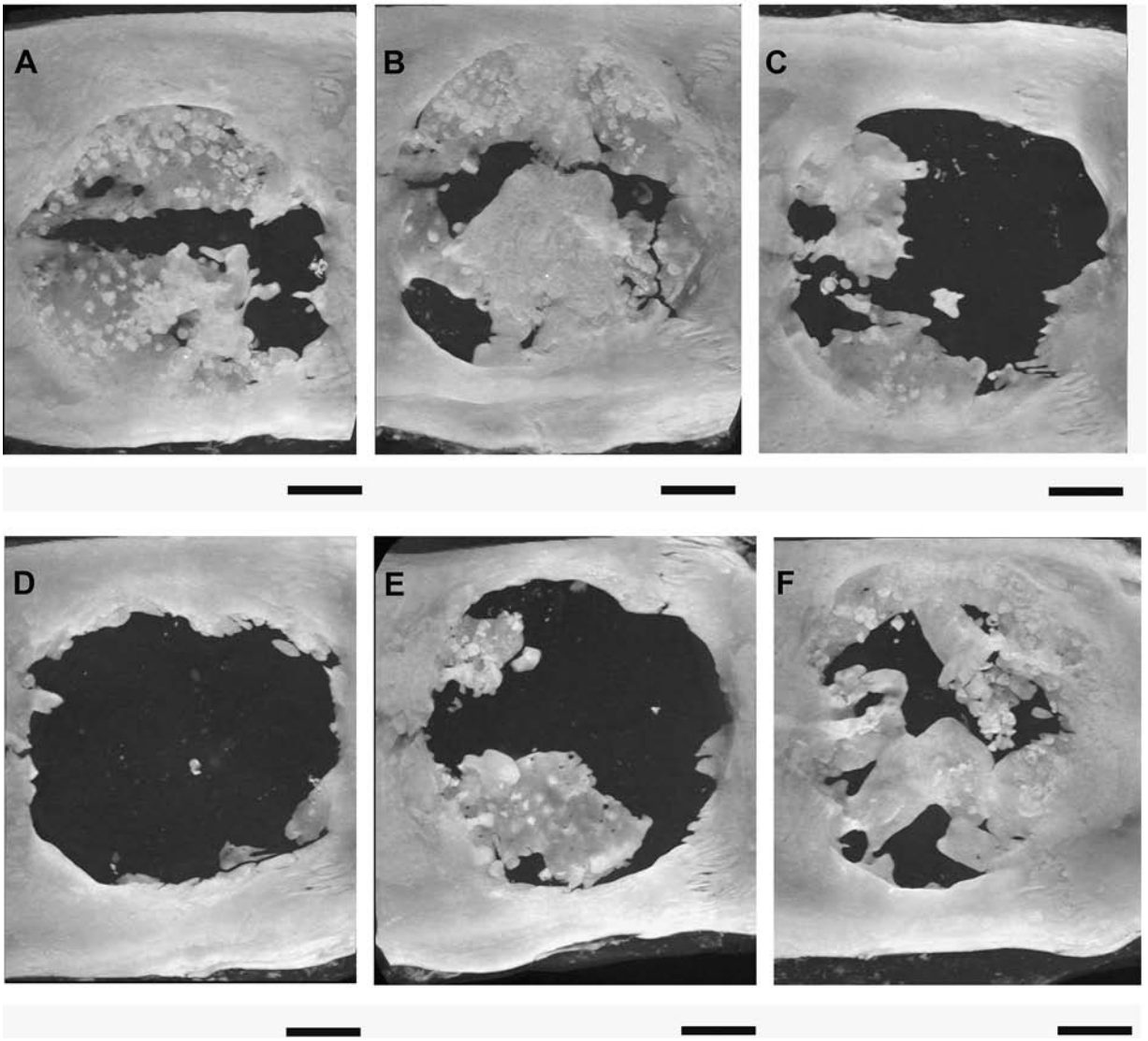

FIG. 5. Examples of micro-CT generated maximum intensity projections of rat cranial defects at 12 weeks. (**A**) Group 1B/0V, Sample #7: bone score = 3, 28.5% bone fill. (**B**) Group 1B/6V, Sample #10: bone score = 4, 40.0% bone fill. (**C**) Group 1B/12V, Sample #22: bone score = 3, 10.9% bone fill. (**D**) Group 0.5B/0V, Sample #31: bone score = 2, 3.1% bone fill. (**E**) Group 0.5B/6V, Sample #41: bone score = 3, 15.1% bone fill. (**F**) Group 0.5B/12V, Sample #49: bone score = 4, 35.0% bone fill. Bars represent 2 mm.

scaffolds. In all samples, the porous PPF scaffolds were visible and intact with no obvious signs of degradation or fracture. The majority of specimens were surrounded by a thin layer of fibrous connective tissue. Unlike the previous study by Patel *et al.*[44] where notable differences in pore tissue response were seen between the groups loaded with 2 μg of BMP-2 (Groups 2B/0V and 2B/12V) and those without BMP-2 (Group 0B/0V and 0B/12V), the pore tissue response among all the groups of this study was quite uniform. The majority of samples had pores mainly filled with immature fibrous tissue containing blood vessels and fibroblasts and a minimal presence of inflammatory cells such as neutrophils or macrophages. Bone formation within the pores or along the dural and periosteal surfaces of the PPF scaffolds was observed more commonly in samples from Group 1B/0V, while the other groups had sporadic bone formation.

Quantitative histological scoring (Fig. 8) correlated well with the trends in the PBF data derived from micro-CT analysis (Fig. 4). When considering the mean scaffold–bone interface score (Fig. 8A), Group 2B/12V (3.0 ± 0.9) was found to have a statistically significantly higher score versus Groups 1B/6V, 1B/12V, 0.5B/0V, and 0.5B/6V (ranging from 2.0 ± 0.0 to 2.2 ± 0.6). This was consistent with the fact that the majority of samples in this study were surrounded by a fibrous capsule and received a scaffold–bone interface score of 2 on histological examination. Pore tissue response (Fig. 8B) also showed a similar trend, with Group 2B/0V (2.8 ± 0.9) having a significantly higher score than Groups 1B/6V, 1B/12V, 0.5B/0V, 0.5B/6V, and 0.5B/12V (ranging from 2.0 ± 0.2 to 2.2 ± 0.4). In addition, Group 1B/0V (2.7 ± 1.0) was observed to have a significantly higher pore response score than Group 0.5B/0V (2.0 ± 0.3). This was also

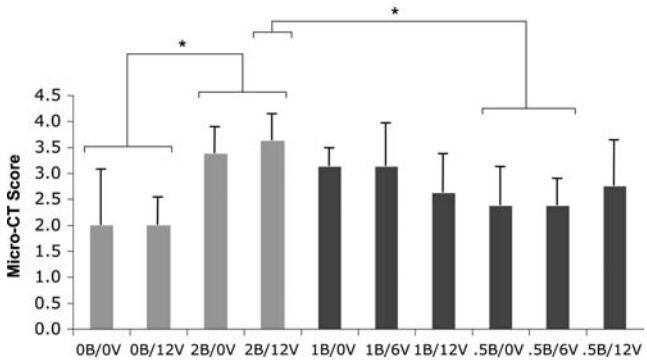

FIG. 6. Average bone score within the defect at 12 weeks as measured by blinded observers assessing maximum intensity projections of micro-CT datasets. Values are given for bone score of the groups performed by Patel *et al.*[44] (Groups 0B/0V, 0B/12V, 2B/0V, and 2B/12V) and this current study (Groups 1B/0V, 1B/6V, 1B/12V, 0.5B/0V, 0.5B/6V, and 0.5B/12V). Error bars represent means ± standard deviation for $n = 8$–9. Statistically significant differences ($p < 0.05$) are denoted by asterisks (*).

consistent with the qualitative histological findings, which showed the majority of implants in this study containing mainly immature fibrous tissue within the pores and minimal bone formation, with Group 1B/0V having more samples with moderate bone formation.

Discussion

Bone regeneration is a complex process involving the coordinated spatio-temporal expression of a multitude of growth factors. Thus, effective bone tissue engineering strategies may require the controlled delivery of multiple growth factors at specific rates. The present study first examined if using growth factor loading doses of relevance to the planned *in vivo* work (i.e., VEGF at 4.8 μg/mg GMPs or BMP-2 at 0.8 μg/mg GMPs) would affect the *in vitro* release kinetics as compared to previous studies that used loading doses in the range of 6–60 ng VEGF or BMP-2 per mg of GMPs.[45,46] The study's main aim was to evaluate the osteogenic response to varied doses of both VEGF and BMP-2, simultaneously delivered within a rat cranial CSD over 12 weeks. Specifically, it was hypothesized that by decreasing the amount of BMP-2 from 2 μg in previous work[44] to 0.5–1 μg in this study, a dose-dependent decrease in bone formation would be seen at 12 weeks. It was also theorized that the addition of VEGF in amounts of 6–12 μg would counter this decrease in bone formation through the promotion of angiogenesis and the recruitment and differentiation of osteoprogenitor cells.

In the first part of this study, the *in vitro* release kinetics of radiolabeled VEGF or BMP-2 from GMPs only and from porous PPF scaffolds incorporating GMPs were examined. For VEGF release, acidic GMPs crosslinked with 10 mM glutaraldehyde were loaded with VEGF, while PBS-loaded basic GMPs crosslinked with 40 mM glutaraldehyde were included as well to simulate the composition of GMPs used for the subsequent *in vivo* study. The BMP-2 release study utilized samples of BMP-2–loaded basic GMPs crosslinked with 40 mM glutaraldehyde combined with PBS-loaded acidic GMPs crosslinked with 10 mM glutaraldehyde.

As in previous studies of *in vitro* VEGF release kinetics,[45] a large burst release was observed in Groups G/V and PG/V during the first 24 h, which can be attributed to the loss of uncomplexed VEGF from the gelatin microspheres.[55] Subsequently, the VEGF release rate over Phases 2–4 (Table 5) showed a significant decline in both groups, suggesting a slower rate of VEGF release as the gelatin microspheres degraded through enzymatic hydrolysis.[55] While the cumulative BMP-2 releases from Groups G/B and PG/B were less than that of the VEGF releasing samples in this study, their release curves were similar to those observed in previous work.[46] Similar to the VEGF releasing groups, Groups G/B and PG/B exhibited increased rates of release in the first 24 h, followed by diminished BMP-2 release over Phases 2–4 due to the initial loss of uncomplexed growth factor, followed by slower release of BMP-2 through enzymatic GMP degradation.

Direct comparison of the release kinetics for Group G/V or G/B to that previously seen from 10 mM acidic GMPs[45] or 40 mM basic GMPs[46] is not possible because this current study utilized a mixture of acidic and basic GMPs for Groups G/V and G/B. Comparison of Group PG/V with the 10 mM GMP composite from previous work[45] or Group PG/B with the 40 mM GMP composite studied previously[46] is somewhat more feasible, because the make-up of the composites and the nature of the release buffer are identical.

However, a difference exists between the two composite scaffolds in the loading doses of growth factor used: past work utilized either 150 ng of VEGF loaded in 2.5 mg of acidic GMPs per composite[45] or 150 ng of BMP-2 loaded in 2.5 mg of basic GMPs per composite.[46] In contrast, this current *in vitro* study utilized growth factor loading concentrations similar in magnitude to previous *in vivo* work,[44] which was either 6 μg of VEGF in 1.25 mg of acidic GMPs per composite or 1 μg of BMP-2 in 1.25 mg of basic GMPs per composite. A higher Phase 1 release rate was observed for the VEGF-releasing composite in this current study (79.9 ± 5.1%/day) versus the previous study (69.5 ± 2.6%/day),[45] suggesting that by increasing the VEGF loading dose by 200 times, a greater proportion of the initial VEGF dose remained uncomplexed. This may have contributed to the release of a greater percentage of VEGF in the first 24 h, before any substantial enzymatic gelatin degradation. Interestingly, a similar Phase 1 release rate was observed for the BMP-2–releasing composite in this study (19.7% ± 8.0%/day) as compared to previous work (17.8% ± 6.1%/day),[46] despite the higher growth factor concentration loaded into the GMPs. This could most likely be attributed to the fact that Group PG/B was centrifuged down at each time point, before the aspiration of supernatant for radioactivity testing, which reduced the chances of accidentally collecting stray GMPs. Prior studies did not centrifuge the composites before supernatant collection at each time point.

A statistically significant effect of vehicle type (i.e., GMPs only vs. composite) on % cumulative release was observed for both VEGF and BMP-2. As seen in Table 5, VEGF release rate differed significantly between the two groups for Phases 1 and 2, suggesting a larger percentage of uncomplexed VEGF was released from composite scaffolds versus GMPs only. A similar trend was observed for BMP-2 release (Table 6). While the mechanism for this difference is unclear, issues such as the interaction between the Pluronic F127 and growth factor-loaded GMPs in the composite scaffolds, as

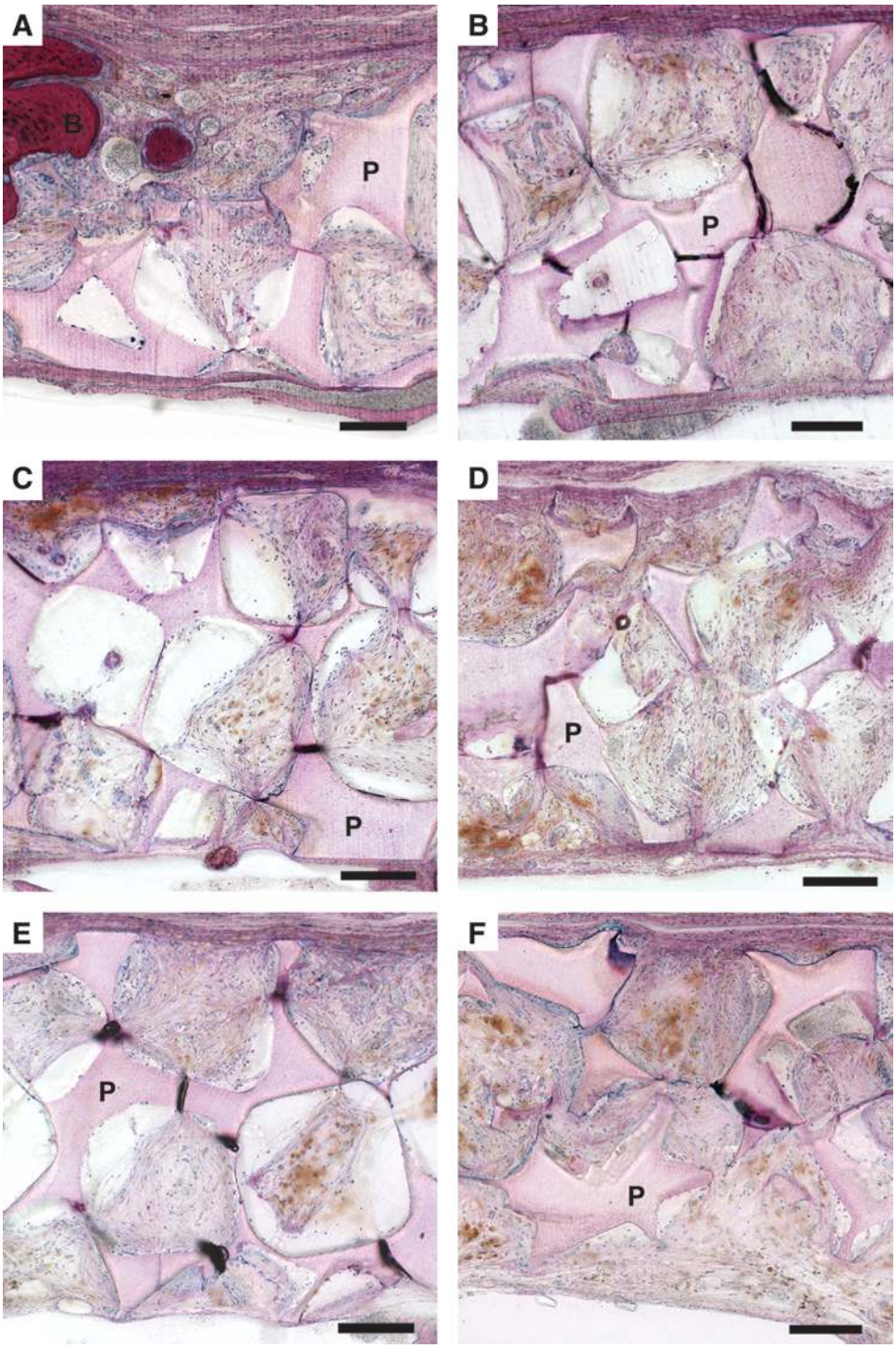

FIG. 7. Representative histological sections of samples from (**A**) Group 1B/0V, (**B**) Group 1B/6V, (**C**) Group 1B/12V, (**D**) Group 0.5B/0V, (**E**) Group 0.5B/6V, and (**F**) Group 0.5B/12V. Note the pores in all groups are mainly filled with fibrous tissue, with a minimal amount of inflammation or bone formation. P, PPF scaffold; B, new bone. Bar represents 200 μm for all panels.

well the differences in handling between the two groups at each time point measurement (i.e., centrifugation of the Group G/V vs. noncentrifugation of Group PG/V), should be taken into consideration. Further conclusions on the appropriateness of the *in vitro* VEGF and BMP-2 release kinetics for *in vivo* applications are not possible because previous work in our laboratory has shown that *in vitro* release kinetics differ from *in vivo* release kinetics.[45,46] Nonetheless, the early VEGF and late BMP-2 release profiles observed in this current study correlate well with the typically early expression of VEGF and later BMP-2 expression during osteoprogenitor cell differentiation *in vitro*[56] and bone healing *in vivo*.[57,58]

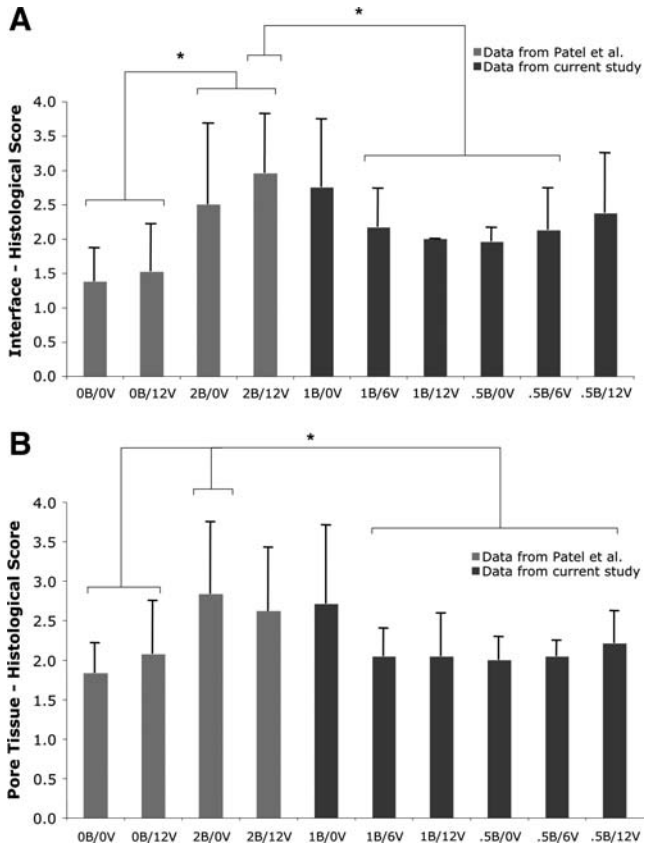

FIG. 8. Average score for (**A**) the hard tissue response at the scaffold–bone interface, and (**B**) the tissue response within the scaffold pores within the defect at 12 weeks as measured by blinded observers assessing histological sections. Values are given for bone score of the groups performed by Patel *et al.*[44] (Groups 0B/0V, 0B/12V, 2B/0V, and 2B/12V) and this current study (Groups 1B/0V, 1B/6V, 1B/12V, 0.5B/0V, 0.5B/6V, and 0.5B/12V). Note for Figure 8B that a significant difference also exists between Groups 1B/0V and 0.5B/0V. Error bars represent means ± standard deviation for $n = 8$–9. Statistically significant differences ($p < 0.05$) are denoted by asterisks (*).

The *in vivo* part of this current study utilized a rat cranial CSD to address the dose effect of BMP-2 and VEGF on bone formation at 12 weeks. Previous work in our laboratory[44] found no significant difference in PBF at 12 weeks between groups implanted with 2 μg of BMP-2 (referred to as Group 2B/0V) and those implanted with 2 μg of BMP-2 and 12 μg of VEGF (i.e., Group 2B/12V). There was, however, a significant difference in PBF between those particular formulations at 4 weeks, indicating that the beneficial effect of dual growth factor release occurred somewhere between 4 and 12 weeks.

To take advantage of using the data from this previous study for comparison (i.e., Groups 0B/0V, 0B/12V, 2B/0V, and 2B/12V), this current study utilized the same surgeon (S.Y.), animal subjects (male Fischer-344 rats), implant vehicle (porous PPF scaffolds incorporating GMPs), and concentration of growth factor per mg of loaded GMP (i.e., 0.8 μg BMP-2 per 1 mg of 40 mM basic GMPs or 4.8 μg of VEGF per 1 mg of 10 mM acidic GMPs). The porous PPF scaffolds used in this study had an average pore size of 300–500 μm, a porosity of 77.9 ± 2.1% and a pore interconnect size between 192 and 224 μm, well above the minimum pore size recommended for bone tissue engineering applications.[59]

It was hypothesized for this current study that by decreasing the dose of BMP-2 delivered, bone formation at 12 weeks would decrease in a dose-dependent fashion, but the addition of VEGF would reverse this effect. Both % bone formation (performed by software) and bone formation scoring (performed by blinded observers) were used to assess bone healing. A statistically significant drop in PBF was observed between Group 2B/0V (37.4 ± 18.8%) and Groups 1B/0V (19.4 ± 7.5%) and 0.5B/0V (6.2 ± 4.9%) (Fig. 4), suggesting a dose-dependent decrease in PBF as the total loading dose of BMP-2 decreased from 2 μg to 0.5–1 μg. Group 2B/0V did not have a statistically significantly different micro-CT bone score from Groups 1B/0V or 0.5B/0V (i.e., 3.4 ± 0.5 vs. 3.1 ± 0.4 and 2.4 ± 0.7, respectively). However, a dose-dependent decrease in the number of samples per group that exhibited bony bridging was observed: Group 2B/0V had 3/8 bridged, while Group 1B/0V had 1/8 bridged, and Group 0.5B/0V did not have any samples exhibiting defect bridging. A similar trend was observed with the histological scoring of the pore tissue response, with a statistically significant decrease in score from Group 2B/0V (2.8 ± 0.9) to Group 0.5B/0V (2.0 ± 0.3) and from Group 1B/0V (2.7 ± 1.0) to Group 0.5B/0V.

Cowan *et al.*[42] examined the bone healing response to a range of BMP-2 doses (30–240 ng/mm^3) coated onto porous PLGA scaffolds within a 5 mM rat cranial defect. Using micro-CT, these authors found a dose response effect on new bone area at 12 weeks. In addition, the smallest BMP-2 dose of 30 ng/mm^3 was found to have a statistically significant difference in % bone fill versus the empty control (i.e., ~58% vs. ~15%). In this current study, Groups 2B/0V, 1B/0V, and 0.5B/0V had BMP-2 concentrations of 40, 20, and 10 ng/mm^3, respectively. The PBF or micro-CT bone scores for Groups 1B/0V and 0.5B/0V were not statistically significantly different, nor were these two groups significantly different from the blank control Group 0B/0V, suggesting the threshold dose for BMP-2–induced bone formation using this particular animal model and release vehicle is between 20 and 40 ng/mm^3.

While a dose-dependent decrease in bone healing was observed among the BMP-2-only control groups, the addition of 6–12 μg of VEGF did not seem to have a beneficial effect on % bone formation or micro-CT bone score. Statistical analysis found that the BMP-2 dose had an effect on PBF ($p < 0.0001$) and micro-CT bone score ($p < 0.0001$), while VEGF dose did not ($p = 0.9495$ for PBF and $p = 0.6488$ for micro-CT bone score). Specifically, there were no statistically significant differences among the following for % bone formation (Fig. 4): (1) Group 2B/0V versus Group 2B/12V, (2) Group 1B/0V vs. 1B/6V vs. 1B/12V, and (3) Group 0.5B/0V vs. 0.5B/6V vs. 0.5B/12V. In each of these three comparisons, the addition of VEGF did not result in a statistically significant increase in % bone formation versus the BMP-2-only control, nor was the PBF for the groups performed in this current study statistically significantly different than the blank control Group 0B/0V. Similar results were seen for the evaluation of micro-CT bone score, such that no statistically significant increase in bone score was observed as 6 or 12 μg VEGF was added to either 0.5 or 1 μg of BMP-2 (Fig. 6).

Histological examination of the samples confirmed these findings with the majority of the samples in this study (i.e., from Groups 1B/6V, 1B/12V, 0.5B/0V, 0.5B/6V, and 0.5B/12V) displaying minimal bone formation within the pores, and instead containing mainly immature fibrous tissue with minimal inflammation.

Interestingly, although PBF and micro-CT bone score did not show improvement with the addition of VEGF to the BMP-2-only controls, there were some inconsistent but noticeable trends in the number of samples per group displaying defect bridging. As shown previously,[44] Group 2B/0V had 3/8 samples bridged, while Group 2B/12V had 5/8 samples bridged. In this current study, Group 1B/0V had 1/8 samples bridged and Group 1B/6V had 3/8 samples bridged. Additionally, Group 0.5B/0V had no samples bridged, but Group 0.5B/12V had 2/8 samples bridged. However, there was no clear trend to this effect, because VEGF loaded groups such as Groups 1B/12V and 0.5B/6V had no samples bridged.

These data suggest an unclear long-term (i.e., 12 weeks postimplantation) effect to the combined delivery of VEGF and BMP-2 versus BMP-2 alone, using this particular animal model and delivery vehicle, at the loading doses chosen. While the benefit of BMP-2 delivery for bone regeneration has been clearly established in the literature, there is still a paucity of data concerning the benefits of multi-growth factor controlled release in this area.

Previous studies have combined BMP-2 with TGF-β3,[43,60] FGF-2,[61] or VEGF,[34,44,62] using a variety of animal models and delivery systems, with mixed results. Oest *et al.*[60] implanted poly(L-lactide-*co*-D,L-lactide) scaffolds containing BMP-2 (200 ng) and TGF-β3 (20 ng) into a rat segmental defect. The authors found no significant difference in bone formation at 4 or 16 weeks between growth factor-enhanced scaffolds versus blank scaffolds. Akita *et al.*[61] used a 4 mM rat cranial defect model to compare groups implanted with a gelatin sponge containing PBS-only, human mesenchymal stem cells (hMSCs), or hMSCs with 10 μg BMP-2 and 10 μg FGF-2. At 4 weeks, the group with hMSCs + growth factors had significantly higher bone mineral density versus the PBS-only and hMSC-only groups, although no significant differences were found at 8 weeks. Neither of these two studies compared dual growth factor delivery to single growth factor delivery.

In contrast, previous studies examining the effect of BMP-2 and VEGF combined delivery have included groups with either BMP-2-only or VEGF-only for comparison. Kakudo *et al.*[62] implanted collagen disks containing either 2 μg of BMP-2 (96 ng/mm^3) alone, or 2 μg BMP-2 and 1 μg of VEGF (48 ng/mm^3) into a rat ectopic bone formation model. At 3 weeks, the BMP-2 + VEGF group had significantly greater bone area and capillary density than BMP-2 alone. Peng *et al.*[34] used an orthotopic bone model to show the beneficial effect of combining VEGF and BMP-2. In one part of that study, the authors implanted cell-impregnated gelatin disks into a 6 mM rat cranial defect. The disks contained transduced MDSCs expressing either BMP-2 (250 ng/10^6 cells/24 h) or VEGF (200 ng/10^6 cells/24 h). At 3 and 6 weeks postimplantation, defects containing implants with both BMP-2 and VEGF expressing cells were found to have a significantly higher relative bone density than those containing either BMP-2–expressing cells only, or VEGF expressing cells only. Further, that same study found an inverse relationship between the degree of bone healing and ratio of VEGF to BMP-2, such that a VEGF:BMP-2 ratio of 1:5 exhibited greater bone area at 3 weeks versus ratios of 1:1 or 5:1, although the differences were not significant.

The studies by Peng *et al.*[34] and Kakudo *et al.*[62] seem to suggest that the combination of BMP-2 and VEGF provides bone tissue engineering constructs with increased osteogenic potential over BMP-2 or VEGF alone. Although such benefits were not observed in the current study, it should be noted that these aforementioned studies utilized different: (1) doses of growth factor, (2) delivery vehicles (i.e., growth factor-impregnated collagen disks or transduced cells), (3) *in vivo* models (i.e., muscle pouch or 6 mM cranial defect), (4) assessment time points (i.e., 3 or 6 weeks), and (5) assessment methods (i.e., radiographic bone mineral density or histologic measures of bone area). Further, it should be reiterated that previous work in our laboratory[44] showed a statistically significant increase in bone formation for Group 2B/12V versus Groups 2B/0V, 0B/12V, and 0B/0V at 4 weeks, while the aim of this present study was to examine longer-term bone regeneration at 12 weeks.

The results of this current study suggest that doses of 0.5–1 μg of BMP-2 (i.e., 10–20 ng/mm^3) released from 40 mM basic GMPs were insufficient to regenerate a significant amount of bone in a critical-size rat cranial defect at 12 weeks, while 2 μg of BMP-2 (40 ng/mm^3) was able to overcome this threshold. Regardless of a BMP-2 loading dose of 0.5, 1, or 2 μg, the addition of 6–12 μg of VEGF (i.e., 119–239 ng/mm^3) released from 10 mM acidic GMPs did not result in a significant increase in percentage bone formation or bone score over BMP-2 alone. In certain instances, however, a larger number of samples per group exhibited bony bridging when VEGF was combined with BMP-2 versus BMP-2 alone, illustrating the need to use both quantitative and qualitative methods of assessment for bone healing.

Given that VEGF plays an early role in bone repair through its involvement with angiogenesis, it is less likely that the release kinetics of VEGF from 10 mM acidic GMPs were suboptimal, considering its *in vitro* (Fig. 2) and *in vivo*[45] release profiles. A lack of VEGF bioactivity was also less of a concern because previous work has documented the *in vitro* bioactivity of VEGF released from GMPs.[45] Although a weakness of this study may be that VEGF bioactivity was not assessed by blood vessel quantification of histological samples at 12 weeks, the main focus of this study was to evaluate the effects of VEGF and BMP-2 on bone formation. Nonetheless, it is possible that an overly large burst release may have resulted in insufficient amounts of VEGF present at later time points to sustain the immature vessel network, resulting in the pruning of unstable vessels.[63] In fact, studies that have utilized VEGF controlled release systems and observed increases in bone formation over controls have used more sustained release profiles.[17]

Consideration should also be given to previous studies[34,62] which used VEGF/BMP-2 ratios of less than 1. In comparison, the VEGF/BMP-2 ratios utilized in this current study (i.e., ranging from 24:1 to 6:1) may have resulted in suboptimal bone formation due to excess VEGF pushing stem cells within the healing defect towards an endothelial lineage, and reducing the number of cells available for osteogenic differentiation.[64]

A final possibility as to why the simultaneous release of VEGF and BMP-2 was not shown to increase PBF over BMP-2 alone, is that adequate vascularization may not be a limiting factor for bone regeneration in the rat critical-size cranial defect model.[42] The abundant vascularity present in the overlying tissues for this particular bone defect model, combined with the ability of BMP-2 to stimulate angiogenesis through VEGF expression in both osteoblasts and endothelial cells[36] may have actually rendered the addition of VEGF as superfluous.

Conclusions

Effective bone tissue engineering strategies may require the ability to recapitulate the natural bone healing environment through the controlled release of multiple growth factors. The field of dual growth factor controlled release, however, is still relatively new and various combinations of angiogenic and osteogenic growth factors are currently under investigation. The first part of this study showed that vehicles loaded with VEGF doses of relevance to *in vivo* applications exhibit a relatively large burst release in the first 24 h, indicative of a large release of uncomplexed VEGF. This was followed by a significantly decreased release rate over the remaining 27 days, characteristic of the enzyme-mediated hydrolysis of GMPs. While *in vitro* BMP-2 release from composites also had a significantly higher Phase 1 release rate than subsequent phases, BMP-2 had a more sustained release profile overall versus VEGF. This study also investigated the dose effect of BMP-2 and VEGF, simultaneously delivered in a rat critical-size cranial defect. It was hypothesized that decreased amounts of BMP-2 from previous *in vivo* work would result in a dose-dependent decrease in bone formation in the BMP-2-only control groups, and that this reduction in bone formation could be reversed by the addition of increasing amounts of VEGF. At 12 weeks, a dose-dependent decrease in bone formation was observed for decreasing loading doses of BMP-2 from 2 μg to 0.5–1 μg. The addition of 6–12 μg of VEGF to the BMP-2-only formulations did not result in a significant increase in percentage bone formation or micro-CT bone score, although an increase in the proportion of bridged defects was noted for certain dual release groups. These results suggest that there is no consistent, observable benefit to the controlled, simultaneous release of BMP-2 and VEGF over BMP-2 alone, for this particular release system and set of loading doses after 12 weeks. Given the small number of studies which have examined the effectiveness of controlled, simultaneous BMP-2 and VEGF release, further investigations are required to determine the optimal loading dose, growth factor ratio, and release kinetics of these cytokines for long term, effective bone regeneration.

Disclosure Statement

To the best of our knowledge, there are no competing financial interests.

References

1. Geiger, M., Li, R.H., and Friess, W. Collagen sponges for bone regeneration with rhBMP-2. Adv Drug Deliv Rev **55,** 1613, 2003.
2. Silva, R.M., Elvira, C., Mano, J.F., San Roman, J., and Reis, R.L. Influence of beta-radiation sterilisation in properties of new chitosan/soybean protein isolate membranes for guided bone regeneration. J Mater Sci Mater Med **15,** 523, 2004.
3. Takahashi, Y., Yamamoto, M., Yamada, K., Kawakami, O., and Tabata, Y. Skull bone regeneration in nonhuman primates by controlled release of bone morphogenetic protein-2 from a biodegradable hydrogel. Tissue Eng **13,** 293, 2007.
4. Shi, X., Sitharaman, B., Pham, Q.P., Liang, F., Wu, K., Billups, W.E., Wilson, L.J., and Mikos, A.G. Fabrication of porous ultra-short single-walled carbon nanotube nanocomposite scaffolds for bone tissue engineering. Biomaterials **28,** 4078, 2007.
5. Shea, L.D., Wang, D., Franceschi, R.T., and Mooney, D.J. Engineered bone development from a pre-osteoblast cell line on three-dimensional scaffolds. Tissue Eng **6,** 605, 2000.
6. Rai, B., Ho, K.H., Lei, Y., Si-Hoe, K.M., Teo, J., C.M., Yacob, K.B., Chen, F., Ng, F.C., and Teoh, S.H. Polycaprolactone-20% tricalcium phosphate scaffolds in combination with platelet-rich plasma for the treatment of critical-sized defects of the mandible: a pilot study. J Oral Maxillofac Surg **65,** 2195, 2007.
7. Spoerke, E.D., Murray, N.G., Li, H., Brinson, L.C., Dunand, D.C., and Stupp, S.I. Titanium with aligned, elongated pores for orthopedic tissue engineering applications. J Biomed Mater Res A **84,** 402, 2008.
8. Datta, N., Pham, Q.P., Sharma, U., Sikavitsas, V.I., Jansen, J.A., and Mikos, A.G. *In vitro* generated extracellular matrix and fluid shear stress synergistically enhance 3D osteoblastic differentiation. Proc Natl Acad Sci USA **103,** 2488, 2006.
9. Leach, J.K., Kaigler, D., Wang, Z., Krebsbach, P.H., and Mooney, D.J. Coating of VEGF-releasing scaffolds with bioactive glass for angiogenesis and bone regeneration. Biomaterials **27,** 3249, 2006.
10. Ruhe, P.Q., Hedberg, E.L., Padron, N.T., Spauwen, P.H., Jansen, J.A., and Mikos, A.G. Biocompatibility and degradation of poly(DL-lactic-co-glycolic acid)/calcium phosphate cement composites. J Biomed Mater Res A **74,** 533, 2005.
11. Khan, Y.M., Katti, D.S., and Laurencin, C.T. Novel polymer-synthesized ceramic composite-based system for bone repair: an *in vitro* evaluation. J Biomed Mater Res A **69,** 728, 2004.
12. McKay, W.F., Peckham, S.M., and Badura, J.M. A comprehensive clinical review of recombinant human bone morphogenetic protein-2 (INFUSE((R)) Bone Graft). Int Orthop **31,** 729, 2007.
13. Iwakura, A., Tabata, Y., Koyama, T., Doi, K., Nishimura, K., Kataoka, K., Fujita, M., and Komeda, M. Gelatin sheet incorporating basic fibroblast growth factor enhances sternal healing after harvesting bilateral internal thoracic arteries. J Thorac Cardiovasc Surg **126,** 1113, 2003.
14. Nevins, M., Camelo, M., Nevins, M.L., Schenk, R.K., and Lynch, S.E. Periodontal regeneration in humans using recombinant human platelet-derived growth factor-BB (rhPDGF-BB) and allogenic bone. J Periodontol **74,** 1282, 2003.
15. Wang, Y., Wan, C., Szoke, G., Ryaby, J.T., and Li, G. Local injection of thrombin-related peptide (TP508) in PPF/PLGA microparticles-enhanced bone formation during distraction osteogenesis. J Orthop Res **26,** 539, 2008.
16. Dean, D., Wolfe, M.S., Ahmad, Y., Totonchi, A., Chen, J.E., Fisher, J.P., Cooke, M.N., Rimnac, C.M., Lennon, D.P., Caplan, A.I., Topham, N.S., and Mikos, A.G. Effect of transforming growth factor beta2 on marrow-infused foam poly(propylene fumarate) tissue-engineered constructs for the repair of critical-size cranial defects in rabbits. Tissue Eng **11,** 923, 2005.

17. Kaigler, D., Wang, Z., Horger, K., Mooney, D.J., and Krebsbach, P.H. VEGF scaffolds enhance angiogenesis and bone regeneration in irradiated osseous defects. J Bone Miner Res **21,** 735, 2006.
18. Gimbel, M., Ashley, R.K., Sisodia, M., Gabbay, J.S., Wasson, K.L., Heller, J., Wilson, L., Kawamoto, H.K., and Bradley, J.P. Repair of alveolar cleft defects: reduced morbidity with bone marrow stem cells in a resorbable matrix. J Craniofac Surg **18,** 895, 2007.
19. Usas, A., and Huard, J. Muscle-derived stem cells for tissue engineering and regenerative therapy. Biomaterials **28,** 5401, 2007.
20. Peterson, B., Zhang, J., Iglesias, R., Kabo, M., Hedrick, M., Benhaim, P., and Lieberman, J.R. Healing of critically sized femoral defects, using genetically modified mesenchymal stem cells from human adipose tissue. Tissue Eng **11,** 120, 2005.
21. Colton, C.K. Implantable biohybrid artificial organs. Cell Transplant **4,** 415, 1995.
22. Goldstein, A.S., Juarez, T.M., Helmke, C.D., Gustin, M.C., and Mikos, A.G. Effect of convection on osteoblastic cell growth and function in biodegradable polymer foam scaffolds. Biomaterials **22,** 1279, 2001.
23. Folkman, J., and Hochberg, M. Self-regulation of growth in three dimensions. J Exp Med **138,** 745, 1973.
24. Thompson, T.J., Owens, P.D., and Wilson, D.J. Intramembranous osteogenesis and angiogenesis in the chick embryo. J Anat **166,** 55, 1989.
25. Maes, C., Carmeliet, P., Moermans, K., Stockmans, I., Smets, N., Collen, D., Bouillon, R., and Carmeliet, G. Impaired angiogenesis and endochondral bone formation in mice lacking the vascular endothelial growth factor isoforms VEGF164 and VEGF188. Mech Dev **111,** 61, 2002.
26. Geris, L., Gerisch, A., Sloten, J.V., Weiner, R., and Oosterwyck, H.V. Angiogenesis in bone fracture healing: a bioregulatory model. J Theor Biol **251,** 137, 2008.
27. Axelrad, T.W., Kakar, S., and Einhorn, T.A. New technologies for the enhancement of skeletal repair. Injury **38 Suppl 1,** S49, 2007.
28. Hirschi, K.K., Skalak, T.C., Peirce, S.M., and Little, C.D. Vascular assembly in natural and engineered tissues. Ann NY Acad Sci **961,** 223, 2002.
29. Ribatti, D. The crucial role of vascular permeability factor/vascular endothelial growth factor in angiogenesis: a historical review. Br J Haematol **128,** 303, 2005.
30. Deckers, M.M., Karperien, M., van der Bent, C., Yamashita, T., Papapoulos, S.E., and Lowik, C.W. Expression of vascular endothelial growth factors and their receptors during osteoblast differentiation. Endocrinology **141,** 1667, 2000.
31. Li, G., Cui, Y., McIlmurray, L., Allen, W.E., and Wang, H. rhBMP-2, rhVEGF(165), rhPTN and thrombin-related peptide, TP508 induce chemotaxis of human osteoblasts and microvascular endothelial cells. J Orthop Res **23,** 680, 2005.
32. Street, J., Bao, M., deGuzman, L., Bunting, S., Peale, F.V., Jr., Ferrara, N., Steinmetz, H., Hoeffel, J., Cleland, J.L., Daugherty, A., van Bruggen, N., Redmond, H.P., Carano, R.A., and Filvaroff, E.H. Vascular endothelial growth factor stimulates bone repair by promoting angiogenesis and bone turnover. Proc Natl Acad Sci USA **99,** 9656, 2002.
33. Sipola, A., Ilvesaro, J., Birr, E., Jalovaara, P., Pettersson, R.F., Stenback, F., Yla-Herttuala, S., Hautala, T., and Tuukkanen, J. Endostatin inhibits endochondral ossification. J Gene Med **9,** 1057, 2007.
34. Peng, H., Usas, A., Olshanski, A., Ho, A.M., Gearhart, B., Cooper, G.M., and Huard, J. VEGF improves, whereas sFlt1 inhibits, BMP2-induced bone formation and bone healing through modulation of angiogenesis. J Bone Miner Res **20,** 2017, 2005.
35. Bouletreau, P.J., Warren, S.M., Spector, J.A., Peled, Z.M., Gerrets, R.P., Greenwald, J.A., and Longaker, M.T. Hypoxia and VEGF up-regulate BMP-2 mRNA and protein expression in microvascular endothelial cells: implications for fracture healing. Plast Reconstr Surg **109,** 2384, 2002.
36. Deckers, M.M., van Bezooijen, R.L., van der Horst, G., Hoogendam, J., van Der Bent, C., Papapoulos, S.E., and Lowik, C.W. Bone morphogenetic proteins stimulate angiogenesis through osteoblast-derived vascular endothelial growth factor A. Endocrinology **143,** 1545, 2002.
37. Steinbrech, D.S., Mehrara, B.J., Saadeh, P.B., Greenwald, J.A., Spector, J.A., Gittes, G.K., and Longaker, M.T. VEGF expression in an osteoblast-like cell line is regulated by a hypoxia response mechanism. Am J Physiol **278,** C853, 2000.
38. Eckardt, H., Ding, M., Lind, M., Hansen, E.S., Christensen, K.S., and Hvid, I. Recombinant human vascular endothelial growth factor enhances bone healing in an experimental nonunion model. J Bone Joint Surg **87,** 1434, 2005.
39. Murphy, W.L., Simmons, C.A., Kaigler, D., and Mooney, D.J. Bone regeneration via a mineral substrate and induced angiogenesis. J Dent Res **83,** 204, 2004.
40. Bodde, E.W., Boerman, O.C., Russel, F.G., Mikos, A.G., Spauwen, P.H., and Jansen, J.A. The kinetic and biological activity of different loaded rhBMP-2 calcium phosphate cement implants in rats. J Biomed Mater Res A **87,** 780, 2008.
41. Chu, T.M., Warden, S.J., Turner, C.H., and Stewart, R.L. Segmental bone regeneration using a load-bearing biodegradable carrier of bone morphogenetic protein-2. Biomaterials **28,** 459, 2007.
42. Cowan, C.M., Aghaloo, T., Chou, Y.F., Walder, B., Zhang, X., Soo, C., Ting, K., and Wu, B. MicroCT evaluation of three-dimensional mineralization in response to BMP-2 doses *in vitro* and in critical sized rat calvarial defects. Tissue Eng **13,** 501, 2007.
43. Simmons, C.A., Alsberg, E., Hsiong, S., Kim, W.J., and Mooney, D.J. Dual growth factor delivery and controlled scaffold degradation enhance *in vivo* bone formation by transplanted bone marrow stromal cells. Bone **35,** 562, 2004.
44. Patel, Z.S., Young, S., Tabata, Y., Jansen, J.A., Wong, M., and Mikos, A.G. Dual delivery of an angiogenic and an osteogenic growth factor for bone regeneration in a critical size defect model. Bone **43,** 931, 2008.
45. Patel, Z.S., Ueda, H., Yamamoto, M., Tabata, Y., and Mikos, A.G. *In vitro* and *in vivo* release of vascular endothelial growth factor from gelatin microparticles and biodegradable composite scaffolds. Pharm Res **25,** 2370, 2008.
46. Patel, Z.S., Yamamoto, M., Ueda, H., Tabata, Y., and Mikos, A.G. Biodegradable gelatin microparticles as delivery systems for the controlled release of bone morphogenetic protein-2. Acta Biomater **4,** 1126, 2008.
47. Holland, T.A., Tessmar, J.K., Tabata, Y., and Mikos, A.G. Transforming growth factor-beta1 release from oligo(poly (ethylene glycol) fumarate) hydrogels in conditions that model the cartilage wound healing environment. J Control Release **94,** 101, 2004.
48. Shung, A.K., Timmer, M.D., Jo, S., Engel, P.S., and Mikos, A.G. Kinetics of poly(propylene fumarate) synthesis by step polymerization of diethyl fumarate and propylene glycol using zinc chloride as a catalyst. J Biomater Sci Polym Ed **13,** 95, 2002.
49. Timmer, M.D., Ambrose, C.G., and Mikos, A.G. Evaluation of thermal- and photo-crosslinked biodegradable poly

(propylene fumarate)-based networks. J Biomed Mater Res A **66,** 811, 2003.
50. Holland, T.A., Tabata, Y., and Mikos, A.G. *In vitro* release of transforming growth factor-beta1 from gelatin microparticles encapsulated in biodegradable, injectable oligo(poly (ethylene glycol) fumarate) hydrogels. J Control Release **91,** 299, 2003.
51. Greenwood, F.C., Hunter, W.M., and Glover, J.S. The preparation of I-131-labelled human growth hormone of high specific radioactivity. Biochem J **89,** 114, 1963.
52. Feldkamp, L.A., Davis, L.C., and Kress, J.W. Practical cone-beam algorithm. J Opt Soc Am A **1,** 612, 1984.
53. Hacker, M., Ringhofer, M., Appel, B., Neubauer, M., Vogel, T., Young, S., Mikos, A.G., Blunk, T., Gopferich, A., and Schulz, M.B. Solid lipid templating of macroporous tissue engineering scaffolds. Biomaterials **28,** 3497, 2007.
54. van der Lubbe, H.B., Klein, C.P., and de Groot, K. A simple method for preparing thin (10 microM) histological sections of undecalcified plastic embedded bone with implants. Stain Technol **63,** 171, 1988.
55. Young, S., Wong, M., Tabata, Y., and Mikos, A.G. Gelatin as a delivery vehicle for the controlled release of bioactive molecules. J Control Release **109,** 256, 2005.
56. Huang, Z., Nelson, E.R., Smith, R.L., and Goodman, S.B. The sequential expression profiles of growth factors from osteoprogenitors [correction of osteroprogenitors] to osteoblasts *in vitro*. Tissue Eng **13,** 2311, 2007.
57. Lalani, Z., Wong, M., Brey, E.M., Mikos, A.G., and Duke, P.J. Spatial and temporal localization of transforming growth factor-beta1, bone morphogenetic protein-2, and platelet-derived growth factor-A in healing tooth extraction sockets in a rabbit model. J Oral Maxillofac Surg **61,** 1061, 2003.
58. Lalani, Z., Wong, M., Brey, E.M., Mikos, A.G., Duke, P.J., Miller, M.J., Johnston, C., and Montufar-Solis, D. Spatial and temporal localization of FGF-2 and VEGF in healing tooth extraction sockets in a rabbit model. J Oral Maxillofac Surg **63,** 1500, 2005.
59. Karageorgiou, V., and Kaplan, D. Porosity of 3D biomaterial scaffolds and osteogenesis. Biomaterials **26,** 5474, 2005.
60. Oest, M.E., Dupont, K.M., Kong, H.J., Mooney, D.J., and Guldberg, R.E. Quantitative assessment of scaffold and growth factor-mediated repair of critically sized bone defects. J Orthop Res **25,** 941, 2007.
61. Akita, S., Fukui, M., Nakagawa, H., Fujii, T., and Akino, K. Cranial bone defect healing is accelerated by mesenchymal stem cells induced by coadministration of bone morphogenetic protein-2 and basic fibroblast growth factor. Wound Repair Regen **12,** 252, 2004.
62. Kakudo, N., Kusumoto, K., Wang, Y.B., Iguchi, Y., and Ogawa, Y. Immunolocalization of vascular endothelial growth factor on intramuscular ectopic osteoinduction by bone morphogenetic protein-2. Life Sci **79,** 1847, 2006.
63. Benjamin, L.E., Golijanin, D., Itin, A., Pode, D., and Keshet, E. Selective ablation of immature blood vessels in established human tumors follows vascular endothelial growth factor withdrawal. J Clin Invest **103,** 159, 1999.
64. Peng, H., Wright, V., Usas, A., Gearhart, B., Shen, H.C., Cummins, J., and Huard, J. Synergistic enhancement of bone formation and healing by stem cell-expressed VEGF and bone morphogenetic protein-4. J Clin Invest **110,** 751, 2002.

Address correspondence to:
Antonios G. Mikos, Ph.D.
Department of Bioengineering
Rice University
P.O. Box 1892, MS 142
Houston, TX 77251-1892

E-mail: mikos@rice.edu

Received: September 15, 2008
Accepted: January 12, 2009
Online Publication Date: February 24, 2009